Journal of Alloys and Compounds 506 (2010) 956–962

Contents lists available at ScienceDirect

Journal of Alloys and Compounds

journal homepage: www.elsevier.com/locate/jallcom

Glass-crystal transformations in $Se_{80-x}Te_{20}Ag_x$ ($x = 0$, 3, 5, 7 and 9) glasses

S. Faheem Naqvi [a,*], Deepika [a], N.S. Saxena [a,*], Kananbala Sharma [a], D. Bhandari [b]

[a] Semi-conductor & Polymer Science Laboratory, 5-6, Vigyan Bhawan, University of Rajasthan, Jaipur 302055, India
[b] Department of Physics, S.S. Jain Subodh P.G. College, Jaipur 302055, India

ARTICLE INFO

Article history:
Received 16 April 2010
Received in revised form 7 July 2010
Accepted 8 July 2010
Available online 22 July 2010

Keywords:
Amorphous materials
Amorphisation
Kinetics
Phase transition
X-ray diffraction

ABSTRACT

$Se_{80-x}Te_{20}Ag_x$ ($x = 0$, 3, 5, 7 and 9) glassy alloys have been prepared by the conventional melt quenching technique. These samples were structurally characterized using X-ray diffraction. Kinetics of phase transformations of $Se_{80-x}Te_{20}Ag_x$ ($x = 0$, 3, 5, 7 and 9) glassy system has been studied by differential scanning calorimetry (DSC) under non-isothermal conditions at five different heating rates. The DSC traces have been analyzed in terms of activation energy and stability by four models viz. Kissinger, Matusita, Gao-Wang and Augis and Bennett models. Avrami exponent (n), dimensionality of growth (m) and frequency factor have also been determined for a better understanding of growth mechanism. The obtained kinetic parameters indicate that stability of the glassy samples increase with increasing Ag content.

1. Introduction

In the past decades, glasses and glass ceramics have attracted much attention because of their unique properties, such as excellent chemical durability, amazing optical transparency and excellent electrical properties. Recently, a great deal of work has been done in the field of chalcogenide glasses due to their useful applications in solid-state electronics [1–3], infrared optical fibers [4], semiconducting properties [5,6] and in optical recording [7].

Chalcogenide glasses containing Se–Te belonging to VI B group elements are efficient materials for thin film circuits, fabrication of semiconductor devices, transistors and detectors. In Selenium (Se), each atom needs two neighbors to satisfy the valence requirements. This can be achieved either by the formation of small molecules (Se_8) or linear polymeric chains (Se) [8,9]. Selenium (Se) can melt without an appreciable change within these structural units, the required random arrangement of atoms being obtained by breaking of the weak bonding between units. A rearrangement into a crystal structure on cooling is a difficult step, and a glass is easily formed. The properties of amorphous Se (a-Se) and the effect of alloying Te into a-Se have been studied by various workers [8–10]. These studies indicate that when Te is incorporated to amorphous Se, it is dissolved in the Se chains to satisfy its coordination requirements and to form a cross-linked structure, which retards the crystallization probability and enhances thermal stability.

The addition of third element in Se–Te glass converts it into an interesting material and new promising properties of the material are expected [11]. The addition of Silver (Ag) to Se–Te is expected to create the compositional and configurational disorder in the material as compared to binary alloy. Se–Te–Ag chalcogenide glasses exhibit single glass transition temperature and single crystallization temperature, which is the main requirement for good optical recording medium [12]. Therefore, the crystallization kinetics of Ag containing chalcogenide glasses is very important for the development of new and better phase change recording materials.

The increasing use of thermoanalytical techniques such as differential thermal analysis (DTA) or differential scanning calorimetry (DSC) has offered the promise of obtaining useful data on phase transformations with simple methods [13,14]. According to the kinetic view point, when the glass transform into the crystalline state, the rearranged particles have to overcome some potential barriers, such as the activation energy of the crystallization. If the potential barrier is higher, i.e. the activation energy of crystallization is larger, the nucleation and thus the crystallization of the glass is more difficult and the atoms do not have enough time to rearrange themselves, when the glass melt is rapidly quenched. Consequently, a random disordered structure is obtained and this is favorable for glass formation [15].

Many efforts have been made in the recent past to study the kinetics of phase transformation of the chalcogenide glasses. Rocca et al. [16] have investigated the crystallization process on amorphous GeTeSb samples near to eutectic point of $Ge_{15}Te_{85}$. They found that the $Ge_{15}Te_{85}$ glass shows a primary crystallization of Te superimposed with a secondary crystallization of GeTe and the addition of Sb (5 at.%) to the eutectic point of $Ge_{15}Te_{85}$ modifies the

* Corresponding authors. Tel.: +91 141 2704056; fax: +91 141 2704056.
E-mail addresses: faheem.spsl@gmail.com (S.F. Naqvi), n_s_saxena@rediffmail.com (N.S. Saxena).

0925-8388/$ – see front matter © 2010 Elsevier B.V. All rights reserved.
doi:10.1016/j.jallcom.2010.07.128

above mentioned behavior. The crystallization kinetic parameters of $Ge_{22.5}Te_{77.5}$ glass using model-free and model-fitting methods have been studied by Abu El-Oyoun [17]. From the various kinetic parameters, the author reported that the activation energy of crystallization is not constant but varies with the degree of crystallization and temperature. Faisal et al. [18] have studied the kinetics of non-isothermal crystallization of ternary $Se_{80}Te_{20-x}Zn_x$ glasses and found that the glass with 2.5 at.% of Zn is the most stable glass within the series. Bayri et al. [19] have studied the crystallization kinetics of $Fe_{73.5-x}Mn_xCu_1Nb_3Si_{13.5}B_9$ (x = 0, 1, 3, 5, 7) amorphous alloys and concluded that the activation energy increases upto x = 3, and then decreases with increasing Mn content.

The aim of the present paper is to study the kinetics of phase transformations of $Se_{80-x}Te_{20}Ag_x$ (x = 0, 3, 5, 7 and 9) glassy system using differential scanning calorimetry (DSC). The study of kinetics is always connected with the concept of activation energies. The values of these energies are associated with nucleation and growth mechanisms that dominate the divitrification of most of glassy solids [20]. The kinetic parameters such as activation energy of glass transition (E_t), activation energy of crystallization (E_c), Avrami exponent (n) and frequency factor (K_o) and m of both the phase transformations (glass transition and crystallization) have been obtained using theoretical models [21] such as Kissinger, Matusita–Sakka, Gao–Wang and Augis-Bennett model. These parameters have further been utilized to determine the thermal stability of these glasses.

2. Experimental details

$Se_{80-x}Te_{20}Ag_x$ (x = 0, 3, 5, 7 and 9) glassy alloys have been prepared by melt quenching technique. The materials of high purity (99.999%) were weighed according to their atomic weight percentages into a quartz ampoule. The content of the ampoule was sealed in the vacuum of 10^{-6} Torr and heated in a furnace. The temperature of the furnace was raised at a rate of 3–4 K min^{-1} up to 925 °C and kept around that temperature for 12 h.

The ampoule was frequently rocked to ensure the homogeneity of the sample. The molten sample was then rapidly quenched in the ice-cooled water to get glassy state. The amorphous nature of the alloy was ascertained through X-ray diffraction pattern of the samples using Bragg-Brentanno geometry on analytical X'pert Pro diffractometer in 2θ range of 15–60° with Cu K_α radiation source (λ = 1.5406 å). The X-ray tube was operated at 45 kV and 40 mA. The thermal behavior of the samples has been investigated using Rigaku 8230 differential scanning calorimetry (DSC). The accuracy of heat flow measurement is ±0.01 mW and the temperature precision as determined by the microprocessor of the thermal analyzer is ±0.1 K. DSC runs have been taken at five different heating rates, i.e. 10, 20, 30, 40 and 50 K min^{-1} on accurately weighed (10–15 mg) samples taken in aluminum (Al) pans under non-isothermal conditions. The temperature range covered in DSC was from room temperature (300 K) to 450 K.

3. Results and discussion

3.1. Structural and thermal analysis

Fig. 1 shows the X-ray diffraction pattern of as-prepared $Se_{80-x}Te_{20}Ag_x$ (x = 0, 3, 5, 7 and 9) glassy systems at room temperature (293 K). The absence of any sharp peak confirms the amorphous nature of these alloys.

The phase transformations of the samples have been observed through DSC at five different heating rates, i.e. 10, 20, 30, 40 and 50 K/min under non-isothermal conditions. Fig. 2 shows the DSC thermograms of $Se_{80-x}Te_{20}Ag_x$ (x = 0, 3, 5, 7 and 9) glassy samples at a heating rate of 10 K/min as a representative case.

When the sample is heated at a constant heating rate in a differential scanning calorimetry experiment, the glass undergoes structural changes and eventually crystallizes. In addition to the large exothermal crystallization peak, the DSC trace shows an endothermic region before crystallization occurs and is denoted as glass transition region. This calorimetric glass transition is generally considered to occur due to changes in the amorphous structure, which approaches a thermodynamic equilibrium state as the temperature of the system is increased. The DSC traces of all the samples show single glass transition and crystallization, which, confirms the homogeneity of the samples. Table 1 lists the characteristic temperatures of all the samples at a heating rate of 10 K/min.

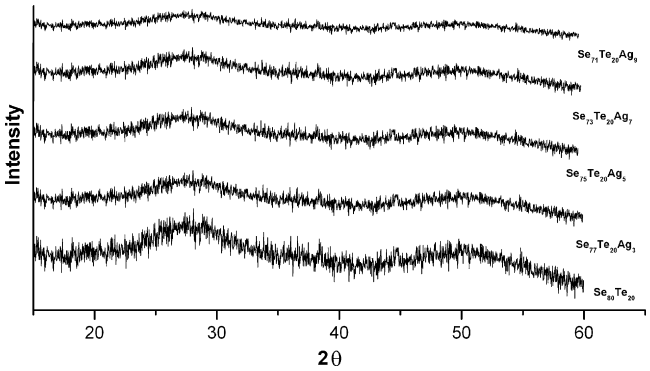

Fig. 1. XRD patterns of $Se_{80-x}Te_{20}Ag_x$ (x = 0, 3, 5, 7 and 9) glassy system.

Table 1
Characteristic temperatures of all the samples at heating rate of 10 K/min.

Sample	T_g (K)	T_c (K)	T_p (K)
$Se_{80}Te_{20}$	341.2	371.1	394.7
$Se_{77}Te_{20}Ag_3$	340.4	370.5	392.9
$Se_{75}Te_{20}Ag_5$	338.0	368.9	390.0
$Se_{73}Te_{20}Ag_7$	342	374.5	395.0
$Se_{71}Te_{20}Ag_9$	343.8	377.5	401.0

From Table 1 and Fig. 2, it is observed that the glass transition temperatures of these samples are found to decrease monotonously up to 5 at. wt% of Ag and then increases on further addition of Ag. A similar trend has also been observed for these samples at other heating rates. The variation of the glass transition temperature of these glasses can be explained on the basis of structural changes due to the introduction of Ag atoms. The generally accepted structural model for a-Se includes [8] two molecular species; meandering chains, which contain helical chains of trigonal Se and Se_8, ring molecules of monoclinic Se. The structure of the Se–Te system prepared by quenching the melt is regarded [22,23] as a mixture of Se_8 rings, Se_6Te_2 rings, and Se–Te copolymer chains. Therefore, an introduction of Te decreases the Se_8 ring concentration favoring Se–Te mixed rings with simultaneous increase in Se and Te atoms in chain structure. When Ag is incorporated, Ag makes bond with Se and is probably dissolved in the Se chains. The number of Se_8 rings

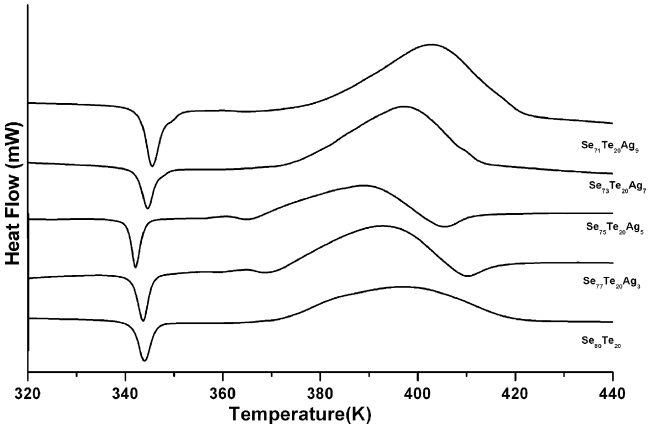

Fig. 2. DSC thermograms of $Se_{80-x}Te_{20}Ag_x$ (x = 0, 3, 5, 7 and 9) glassy system at a heating rate of 10 K/min.

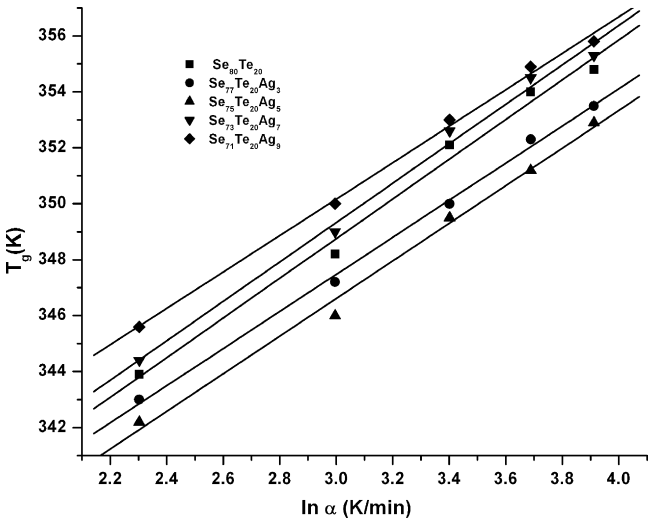

Fig. 3. Variation of T_g with ln(α) of $Se_{80-x}Te_{20}Ag_x$ (x = 0,3,5,7 and 9) glassy system.

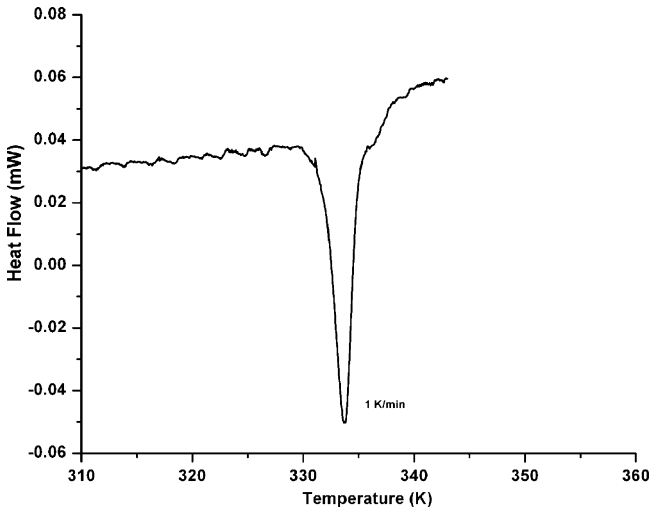

Fig. 4. DSC thermogram of $Se_{71}Te_{20}Ag_9$ glass at 1 K/min.

increases while the number of long Se–Te polymeric chains and Se–Te mixed rings decreases. T_g decreases [24] with increasing ring concentration. This in turn explains the decrease in T_g values with the increase of Ag concentration up to 5 at. wt%. Further, when Ag is added beyond 5 at. wt%, Ag–Se bond formation take place along with Ag–Ag bonds, which results in a decrease of Se_8 rings. The single bond energy values [25,26] of Se–Se and Ag–Ag bonds are 225 and 160 kJ/mol, respectively, while the single covalent bond energies of Se–Te, Ag–Te and Se–Ag are 205.8, 195 and 202.5 kJ/mol, respectively. Since the bonds are formed in sequence of decreasing bond energy until the available valence of the atoms are satisfied, therefore the bond energies are assumed to be additive. Then, the cohesive energies are calculated by summing the bond energies of the bonds present in the material [27]. Hence the formation of Ag–Se and Ag–Ag bond increases the overall cohesive energy of the system which in turns increases the glass transition temperature (T_g). Moreover, the decrease in Se bonds (Se_8 rings) makes the structure more ordered and rigid. This ordered and rigid structure requires higher energy for softening and therefore T_g and T_c are observed at higher temperatures.

3.2. Kinetics of phase transformations

3.2.1. Glass transition region

The glass transition region of a system has been studied in terms of the variation of glass transition temperature with heating rate (α). In addition to this, the activation energy of the glass transition (E_t) has also been evaluated. The glass transition temperature, T_g, represents the strength or rigidity of the glassy alloy [28,29].

The dependence of T_g on heating rate (α) can be discussed on the basis of two approaches. The first approach is the empirical relation suggested by Lasocka [30], which has the form

$$T_g = A + B\ln\alpha \quad (1)$$

where A and B are constants for a given glass composition. The value of A depicts the value of the glass transition temperature (T_g) at heating rate of 1 K/min, while B is proportional to the time taken by the system to reduce its glass transition temperature (T_g), when its heating rate is lowered from 10 to 1 K/min. Fig. 3 depicts the variation of T_g with ln(α) for the investigated $Se_{80-x}Te_{20}Ag_x$ (x = 0, 3, 5, 7 and 9) glassy system.

From Fig. 3 it is found that this equation holds good for investigated samples. The values of A and B for all samples are listed in Table 2. The value of A for $Se_{71}Te_{20}Ag_9$ glass has also been confirmed from the DSC thermogram taken at 1 K/min and has been shown in Fig. 4 as a representative case.

The second approach that shows the dependence of T_g on heating rate is known as the Kissinger formulation [31]. This equation is used for the evaluation of the activation energy for the amorphous glass-transition (E_t), inspite of the fact that this equation is used for the evaluation of the activation energy of the crystallization, it has been frequently used for the determination of the activation energy of glass transition using the peak glass transition temperatures. The Kissinger model is based on peak shift method and if the shift in the glass transition peak with heating rate is similar to peak shifts in the crystallization region, then this equation can be used for the determination of the activation energy of glass transition [32]. This condition is satisfied in the measurements mentioned in this study.

The Kissinger equation relating the peak temperature with heating rate (α) is written as:

$$\frac{\ln\alpha}{T_{gp}^2} = -\left(\frac{E_t}{RT_{gp}}\right) + \text{constant} \quad (2)$$

where E_t is the activation energy of the glass transition, T_{gp} is the peak glass transition temperature, α is the heating rate and R is the universal gas constant. Fig. 5 shows the plot of $\ln(\alpha/T_{gp}^2)$ versus $1000/T_{gp}$ for $Se_{80-x}Te_{20}Ag_x$ (x = 0, 3, 5, 7 and 9) glassy alloys.

The values of activation energies of glass transition (E_t) for all compositions are also listed in Table 2. From Table 2, it is observed that the value of E_t decreases with increase of Ag concentration. This is due to the fact that Se and Te both are twofold coordinated where as Ag is fivefold coordinated. When Ag is introduced into Se–Te system, it tries to satisfy its coordination requirements and bond energy. This gives rise to bond disorder with some degrees of topological disorder which increases the entropy of the system

Table 2
The values of A, B and Activation energy of glass transition (E_t) for $Se_{80-x}Te_{20}Ag_x$ (x = 0, 3, 5, 7 and 9) glassy alloys.

Composition	A (K)	B (min)	Activation energy of glass transition (E_t) (kJ/mol)
			Kissinger Model
$Se_{80}Te_{20}$	327.5	7.02 ± 0.41	148.73 ± 1.01
$Se_{77}Te_{20}Ag_3$	326.2	6.63 ± 1.41	147.97 ± 0.45
$Se_{75}Te_{20}Ag_5$	325.4	6.72 ± 0.31	141.32 ± 0.52
$Se_{73}Te_{20}Ag_7$	328.2	7.04 ± 0.35	137.51 ± 0.87
$Se_{71}Te_{20}Ag_9$	330.6	6.51 ± 1.28	134.68 ± 0.90

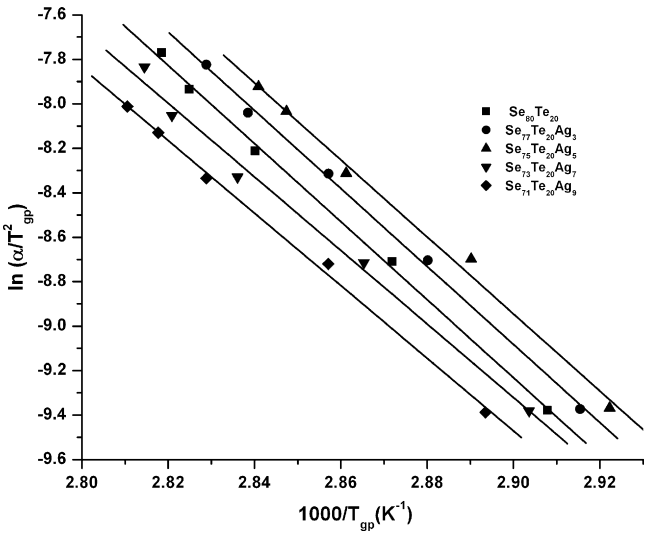

Fig. 5. Plots of $\ln(\alpha/T_{gp}^2)$ against $1000/T_{gp}$ of $Se_{80-x}Te_{20}Ag_x$ ($x = 0, 3, 5, 7$ and 9) glassy system.

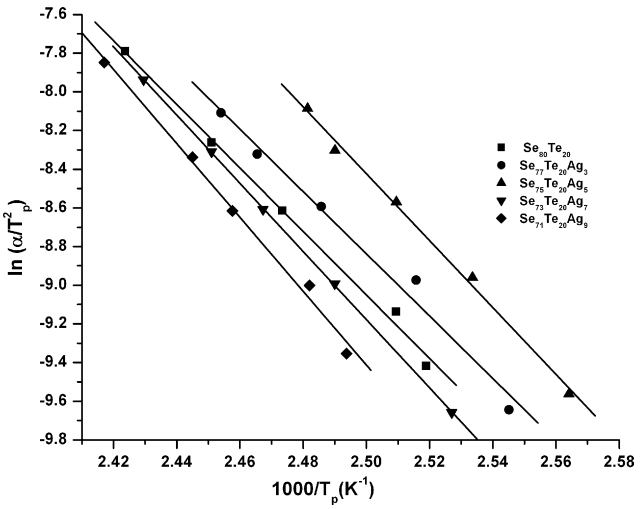

Fig. 6. Variation of $\ln(\alpha/T_p^2)$ with $1000/T_g$ of $Se_{80-x}Te_{20}Ag_x$ ($x = 0, 3, 5, 7$ and 9) glasses.

[33]. Therefore, the internal energy, which arises from the motion of atoms, increases, i.e. the barrier height between two metastable states decreases. The decrease in the barrier height between the adjacent metastable states in the glassy region means that activation energy decreases and a jump to more stable metastable state in this region is preferable. Hence, the decrease in activation energy E_t is due to the increase in the internal energy.

The $Se_{71}Te_{20}Ag_9$ glass is found to possess lowest E_t. It is reported [34,35] that the glass with lower E_t is more stable; therefore, it may be concluded that the stability of the glass increases with the increase in Ag concentration.

3.2.2. Crystallization

The Kinetic analysis of crystallization reaction is related to the knowledge of the reaction rate constant as a function of temperature. The activation energies to be considered in an amorphous–crystalline transformation process are the activation energy for nucleation (E_n) and activation energy for growth (E_g). The activation energy for the whole process is called the activation energy of crystallization and is denoted by (E_c). The thermal analysis methods enable the determination of E_c [36,37].

The activation energies of crystallization (E_c) for $Se_{80-x}Te_{20}Ag_x$ ($x = 0, 3, 5, 7$ and 9) glassy system have been estimated using the following methods.

3.2.2.1. Kissinger model. The activation energies of crystallization (E_c) for $Se_{80-x}Te_{20}Ag_x$ ($x = 0, 3, 5, 7$ and 9) glassy system have been determined using the following equation proposed by Kissinger [31].

$$\ln\left(\frac{\alpha}{T_p^2}\right) = -\left(\frac{E_c}{RT_p}\right) + \text{constant} \tag{3}$$

where T_p is the peak crystallization temperature. Fig. 6 shows the variation of $\ln(\alpha/T_p^2)$ with $1000/T_p$ for $Se_{80-x}Te_{20}Ag_x$ ($x = 0, 3, 5, 7$ and 9) glasses. The data were well-fitted by straight lines. The slope of these straight lines gives the activation energy of crystallization.

3.2.2.2. Matusita and Sakka model. Crystallization kinetics has also been studied using a method suggested specially for non-isothermal experiments by Matusita et al. [38]. The value of fraction crystallized (x), in glass, heated at constant heating rate (α) is related to the effective activation energy of amorphous–crystalline transformation (E_c), through the following expression:

$$\ln[-\ln(1-x)] = -n\ln\alpha - 1.502\,\frac{mE_c}{RT} + \text{constant} \tag{4}$$

where x is the fraction of crystals precipitated in a glass heated at uniform rate and n is a numerical factor depending on the nucleation process. The fraction of volume x crystallized at any temperature T is given as $x = A_T/A$, where A is the total area of the exotherm between temperature T_1 where crystallization just begin and the temperature T_2 where the crystallization is completed. A_T is the area between T_1 and T_2 as shown by the hatched portion in Fig. 7. Here $n = m + 1$ is taken for a quenched glass containing no nuclei and $n = m$ for a preheated glass containing sufficiently large number of nuclei, where m is an integer which represents the dimensionality of growth. Fig. 8 shows the plot of $\ln[-\ln(1-x)]$ against $1000/T$ at five different heating rates 10, 20, 30, 40 and 50 K/min for $Se_{71}Te_{20}Ag_9$ glassy alloy as a representative case. All the other samples of the series also show the same behavior.

At high temperatures or in regions characterized by large crystallization fractions, a nonlinear behavior was seen for all heating rates. A similar behavior has also been reported for other chalcogenide glasses [39,40]. This nonlinear character can be attributed

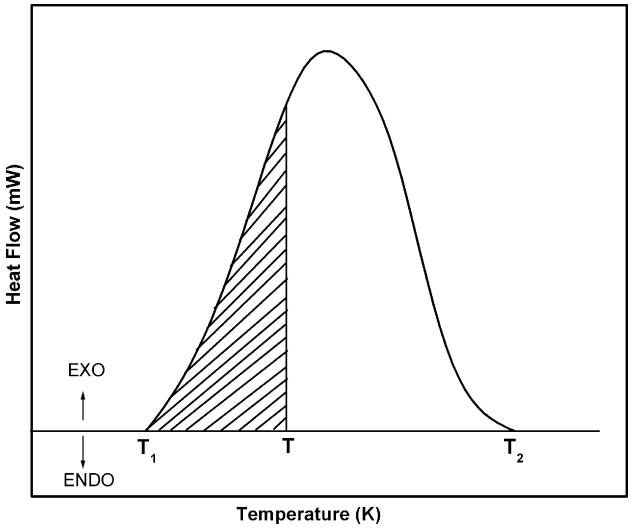

Fig. 7. Typical DSC curve indicating the estimation of volume fraction crystallized.

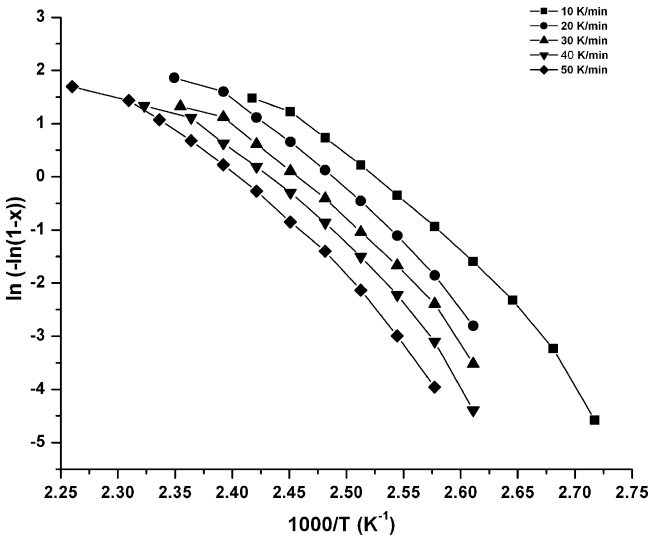

Fig. 8. Variation of $\ln[-\ln(1-x)]$ with $1000/T$ at different heating rates for $Se_{71}Te_{20}Ag_9$ glassy alloy.

to the saturation of nucleation sites in the final stages of crystallization [41] or to the restriction of crystal growth by small size of the particle [42]. From Fig. 8, the value of mE_c was calculated from the slope of the $\ln[-\ln(1-x)]$ versus $1000/T$ for all heating rates.

At constant temperature, Eq. (4) can be written as:

$$\ln[-\ln(1-x)] = -n\ln\alpha + \text{constant} \tag{5}$$

Fig. 9 shows linear plots of $\ln[-\ln(1-x)]$ versus $\ln(\alpha)$ at three fixed temperatures for $Se_{71}Te_{20}Ag_9$ glass. Using Eq. (5), the values of n have been determined from the slopes of these linear plots at each temperature and are given in Table 3 for $Se_{80-x}Te_{20}Ag_x$ ($x = 0$, 3, 5, 7 and 9) glassy system.

As no heat treatment was given to nucleate the sample prior to DSC scans, therefore, n is considered to be equal to $(m+1)$. The values of n are given in Table 3. It is to be noted [43,44] here that if the value of n is less than 2 then the value of m will be 1. Hence the value of the corresponding m is equal to 1. The result indicates that the crystallization process is carried out by surface nucleation with one dimensional growth.

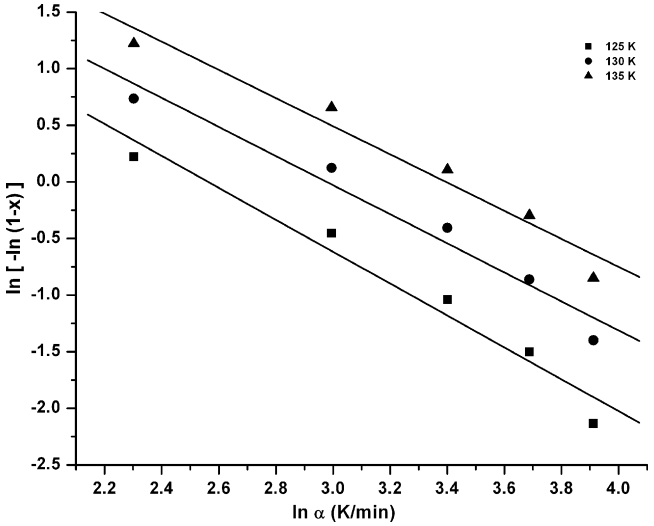

Fig. 9. Variation of $\ln[-\ln(1-x)]$ with $\ln\alpha$ of $Se_{71}Te_{20}Ag_9$ glassy alloy.

Table 3
Values of Avrami exponent and Frequency factor for $Se_{80-x}Te_{20}Ag_x$ ($x = 0$, 3, 5, 7 and 9) glassy alloys.

Sample	Avrami exponent (n)		Frequency factor (K_o)
	Matusita model	Gao Wang model	
$Se_{80}Te_{20}$	1.14	1.14	5.43×10^{20}
$Se_{77}Te_{20}Ag_3$	1.21	0.94	1.71×10^{20}
$Se_{75}Te_{20}Ag_5$	1.55	1.08	5.70×10^{19}
$Se_{73}Te_{20}Ag_7$	1.38	1.03	1.86×10^{18}
$Se_{71}Te_{20}Ag_9$	1.31	1.34	1.28×10^{17}

From the value of n and the average mE_c, the activation energy of crystallization of the $Se_{80-x}Te_{20}Ag_x$ ($x = 0$, 3, 5, 7 and 9) glassy alloys can be calculated.

3.2.2.3. Gao and Wang model. Gao and Wang [45] proposed a slightly different method to analyze DSC thermograms in terms of the activation energy E_c, the dimensionality m, the frequency factor K_o, etc., during the crystallization process. This theory is based on the same fundamental assumption imposed on the Johnson–Mehl–Avrami (JMA) transformation equation. It assumes that the nucleation is randomly distributed and that the growth rate of the new phase depends on the temperature and not on time. The theory provides the relationship between the maximum crystallization rate and peak crystallization temperature, which is given by:

$$\ln\left(\frac{dx}{dt}\right)_p = -\frac{E_c}{RT_p} + \text{constant} \tag{6}$$

where $(dx/dt)_p$ is the rate of volume fraction crystallized at the temperature corresponding to peak of crystallization T_p, which is proportional to the exothermic peak height. Fig. 10 shows the plot of $(dx/dt)_p$ against temperature (T) at different heating rates for $Se_{71}Te_{20}Ag_9$ glass.

It is clear from Fig. 10 that the peak height increases and shifts towards higher temperature values with the increase in the heating rate. Shifting of the crystallization peak towards the higher temperatures is an outcome of the fact that when the heating rate is increased, the larger amount of heat is absorbed by the system per second. The excess heat absorbed over the heat due to smaller heating rate causes the transformation at a higher temperature and hence there is a shift in transition temperatures towards the higher temperatures at higher heating rates. Also the height of the crystallization rate curve with heating rate is explained on the basis of the

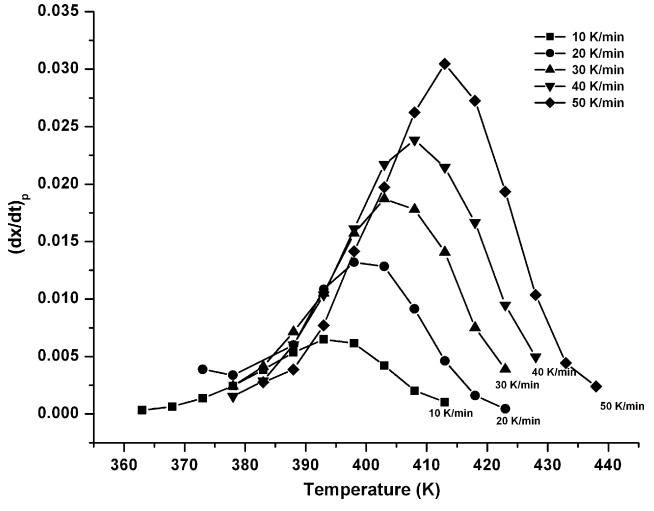

Fig. 10. Variation of $(dx/dt)_p$ with temperature (T) at different heating rates for $Se_{71}Te_{20}Ag_9$ glassy alloy.

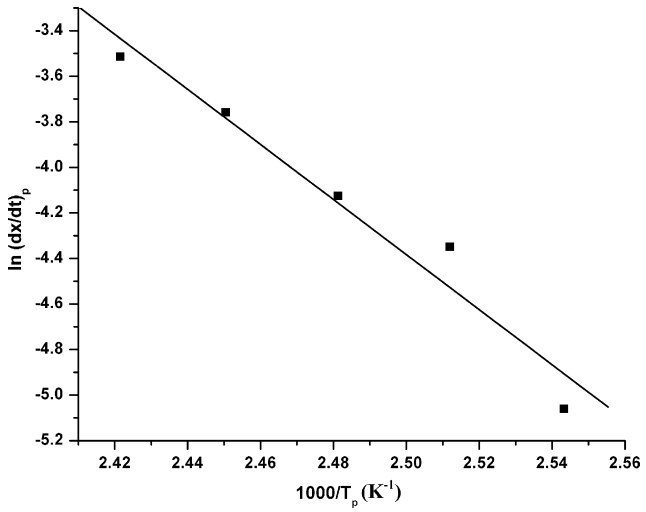

Fig. 11. Variation of $\ln(dx/dt)_p$ with $1000/T$ for $Se_{71}Te_{20}Ag_9$ glassy alloy.

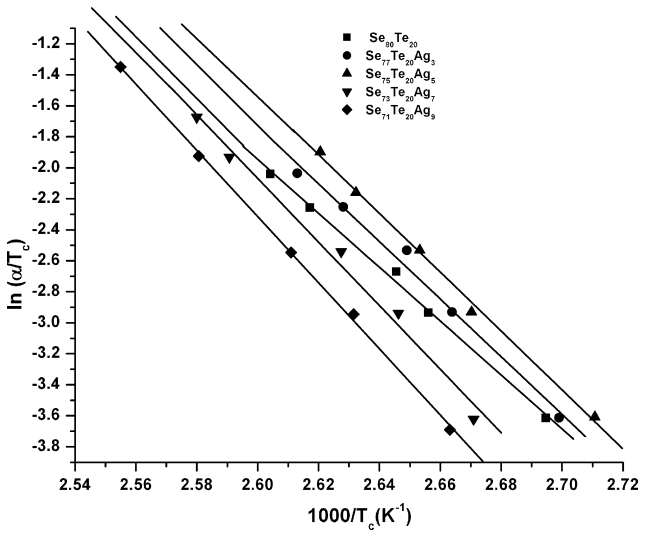

Fig. 12. Variation of $\ln(\alpha/T_c)$ with $1000/T_c$ for $Se_{80-x}Te_{20}Ag_x$ ($x = 0$, 3, 5, 7 and 9) glassy system.

fact that at higher heating rate the volume of fraction crystallized in a given time is more as compared to fraction crystallized in the same time with low heating rate.

Gao and Wang plot ($\ln(dx/dt)_p$ versus $1000/T_p$) for $Se_{71}Te_{20}Ag_9$ glass is shown in Fig. 11 as a representative case. This plot is fitted to straight line and the slope of this straight line gives the activation energy of crystallization (E_c).

The Gao and Wang method is also used to evaluate the Avrami exponent using the following relations:

$$\left(\frac{\alpha E_c}{RT^2}\right) K_p = 1 \tag{7}$$

$$K_p = K_o \exp\left(\frac{-E_c}{RT_p}\right) \tag{8}$$

$$\left(\frac{dx}{dt}\right)_p = 0.37\, n\, K_p \tag{9}$$

The values of Avrami exponent (n) obtained using above relation are shown in Table 3. The value of the corresponding m is equal to 1 for all the samples, suggesting surface nucleation with one-dimensional growth. The values of Avrami exponent (n) and dimensionality of growth (m) obtained from the Gao–Wang and Matusita models are in good agreement with each other.

3.2.2.4. Augis and Bennet model. The activation energy (E_c) of crystallization as well as frequency factor can also be determined by an approximation method developed by Augis and Bennet [46], which is given as follows:

$$\ln\left(\frac{\alpha}{T_c}\right) = \frac{-E_c}{RT_c} + \ln K_o \tag{10}$$

where T_c is the temperature at which the crystallization just begins and K_o is the frequency factor (in s^{-1}). The plots between $\ln(\alpha/T_c)$ and $1000/T_c$ for $Se_{80-x}Te_{20}Ag_x$ ($x = 0$, 3, 5, 7 and 9) glassy system are shown in Fig. 12.

The value of K_o, which is defined as the number of attempts made by the nuclei per second to overcome the energy barrier, can be calculated from the knowledge of $\ln K_o$ from Eq. (10). The values of K_o for all the samples are given in Table 3. These values are indicative of the fact that the barrier to crystallization increases with increase in silver (Ag) content, which in turn decreases the attempts made by the nuclei's to overcome the crystallization barrier. The decrease in number of attempts to cross-crystallization barrier also decreases the tendency of crystallization and hence makes the sample more stable against crystallization. The number of attempts made by the nuclei to cross the barrier and the tendency to crystallization is lowest for $Se_{71}Te_{20}Ag_9$ glass, which indicates the higher stability of this glassy composition. The values of activation energy of crystallization obtained from above discussed theoretical model have been listed in Table 4.

From Table 4, it is clear that the barrier to crystallization increases with the increase in Ag concentration in the samples. This indicates that the atoms require large energy to jump from the glassy state to crystalline state hence the stability increases with increase in Ag concentration in the samples. The difference in the activation energy as calculated with the different models, even for the same sample, may be attributed to the different approximations used in the models. Besides, one of the factors influencing the activation energy may be the temperature gradient, which may not be the same for all heating rates, when the sample is placed in the DSC furnace. This arises due to the error in placing the pan in the DSC furnace with respect to the position of thermocouple. Another factor influencing the activation energy is that the models like Kissinger equation were developed for clays but have been frequently used in literatures [47,48] for determining the activation energy of the glasses.

The Kissinger equation was basically developed for studying the variation of the peak crystallization temperature with heating rate. According to Kissinger's method, the transformation under non-isothermal condition is represented by a first-order (i.e. $n = 1$) reaction. Moreover, the concept of nucleation and growth has not been included in Kissinger equation. Matusita et al. have developed a method on the basis of the fact that crystallization does not advance by an nth-order reaction but by a nucleation and growth process. They emphasized that crystallization mechanisms such as bulk crystallization (bulk nucleation followed by two- or three-dimensional growth) or surface crystallization (bulk nucleation followed by linear growth) should be taken into account for obtaining E_c. In addition to activation energy, Matusita's method provides information about the Avrami exponent and dimensionality of growth. Gao-Wang and Augis-Bennett methods are helpful in obtaining kinetic parameters such as frequency factor (K_o), rate constant (K) along with activation energy of crystallization and therefore preferred for the calculation of the kinetics over the other models.

Thermal stability of $Se_{80-x}Te_{20}Ag_x$ ($x = 0$, 3, 5, 7 and 9) glasses has been ascertained through the $T_c - T_g$ difference. Fig. 13 shows

Table 4
Activation energy of crystallization (E_c) of $Se_{80-x}Te_{20}Ag_x$ (x = 0, 3, 5, 7 and 9) glassy systems using different theoretical models.

Composition	Activation energy of crystallization (E_c)			
	Kissinger model	Matusita model	Augis and Bennet model	Gao and Wang model
$Se_{80}Te_{20}$	116.97 ± 2.96	108.891 ± 1.40	144.49 ± 4.50	90.54 ± 1.20
$Se_{77}Te_{20}Ag_3$	133.8 ± 0.45	114.621 ± 1.63	154.47 ± 1.10	116.48 ± 1.48
$Se_{75}Te_{20}Ag_5$	143.83 ± 1.40	115.24 ± 1.75	157.79 ± 0.60	123.6 ± 6.90
$Se_{73}Te_{20}Ag_7$	146.57 ± 0.20	117.98 ± 1.79	170.60 ± 1.25	128.86 ± 1.38
$Se_{71}Te_{20}Ag_9$	158.78 ± 0.90	120.98 ± 1.90	177.42 ± 1.00	130.9 ± 1.64

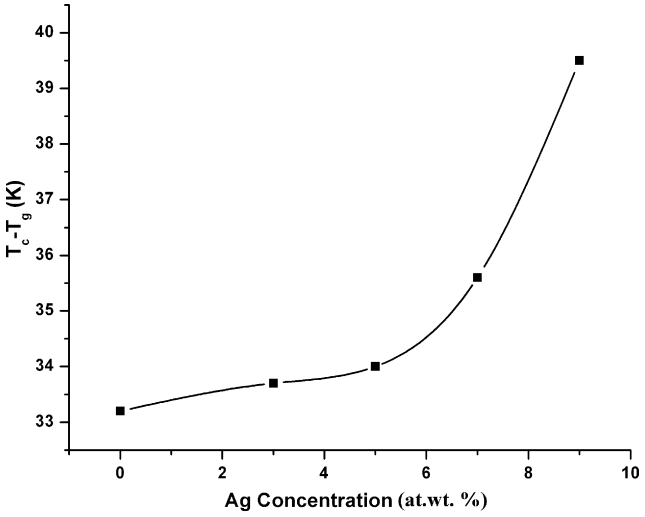

Fig. 13. Plot of $T_c - T_g$ against Ag composition a heating rate of 50 K/min.

a plot of $T_c - T_g$ against the Ag content of the samples at a heating rate of 50 K/min as a representative case. It is clear from Fig. 13 that the value of $T_c - T_g$ increases with the increase in Ag concentration. Therefore, it is again confirmed that the stability increases with the increasing Ag content in the samples.

4. Conclusions

The kinetics of phase transformation of $Se_{80-x}Te_{20}Ag_x$ (x = 0, 3, 5, 7 and 9) glassy system has been carried out using several theoretical models and following conclusions could be made:

1. The glassy alloys under investigation shows single glass transition and crystallization region, confirming the homogeneity of the samples.
2. The lowest value of E_t and the highest value of E_c for $Se_{71}Te_{20}Ag_9$ glassy sample indicate that this glass is more stable as compared to other samples of the series. The values $T_c - T_g$ also confirm the same fact.
3. Besides activation energy, frequency factors (K_o) have also been determined. A decrease in the values of frequency factor (K_o) with increasing concentration of Ag also suggest that stability increases with increasing Ag content in the samples.

Acknowledgements

Authors are thankful to Mr. Mahesh Baboo for his help in various ways during the course of this work. FIST programme in the Department of Physics, University of Rajasthan for using DSC is gratefully acknowledged.

References

[1] Deepika, V.K. Saraswat, P.K. Jain, N.S. Saxena, K. Sharma, T.P. Sharma, S.K. Dhawan, AIP Proc. 1004 (2008) 85.
[2] Am. Abd Elnaeim, K.A. Aly, N. Afify, A.M. Aonsehlly, J. Alloys Compd. 491 (2010) 85.
[3] J. Vazquez, P.L. Lopez-Alemany, P. Villares, R. Jimenez-Garay, J. Alloys Compd. 354 (2003) 153.
[4] H.A. Abd, E.L. Ghani, M.M. abd El Rahim, M.M. Wakkad, A. Abo Sheli, N. Assraan, Physica B 381 (2006) 156.
[5] M.M. Abd El-Raheem, H.M. Ali, J. Non-Cryst. Solids 356 (2010) 77.
[6] E.R. Shaabam, Physica B 373 (2006) 211.
[7] N.A. Hegab, M.A. Afifi, H.E. Atyia, A.S. Farid, J. Alloys Compd. 477 (2009) 925.
[8] G. Lucovsy, Mater. Res. Bull. 4 (1996) 505.
[9] J. Schotmiller, M. Tabak, G. Lucovsy, A. Ward, J. Non-Cryst. Solids 4 (1970) 80.
[10] E. Maruyama, Jpn. J. Appl. Phys. 21 (1982) 213.
[11] N. Mehta, S.K. Arrahari, A. Kumar, Mater. Lett. 61 (3) (2007) 837.
[12] F. Jiang, M. Jiang, L. Hou, F. Gan, M. Okuda, Jpn. J. Appl. Phys. Suppl. 28 (1989) 293.
[13] E.R. Shaaban, M.Y. Hassaan, A.G. Mostafa, A.M. Abdel-Ghany, J. Alloys Compd. 482 (2009) 440.
[14] Deepika, N.S. Saxena, J. Phys. Chem. B 114 (2010) 28.
[15] Deepika, K.S. Rathore, N.S. Saxena, J. Appl. Phys. A 98 (2010) 441.
[16] J. Rocca, M. Erazu, M. Fontana, B. Arcondo, J. Non-Cryst. Solids 355 (2009) 2068.
[17] M. Abu El-Oyoun, J. Alloys Compd. 486 (2009) 1.
[18] A. Faisal, al-Agel, K. Sinha, M. Zulfequar, J. Alloys Compd. 497 (2010) 215.
[19] N. Bayri, T. Izgi, H. Gencer, P. Sovak, M. Gunes, S. Atalay, J. Non-Cryst. Solids 355 (2009) 12.
[20] P. Pradeep, N.S. Saxena, M.P. Saxena, A. Kumar, Phys. Scr. 54 (1996) 207.
[21] G. Kaur, T. Komatsu, R. Thangaraj, J. Mater. Sci. 35 (2000) 903.
[22] K. Shimakawa, S. Nitta, Phys. Rev. B 17 (1978) 3950.
[23] R.M. Mehra, G. Kaur, P.C. Mathur, J. Mater. Sci. 26 (1991) 3433.
[24] A. Eisenberg, Polym. Lett. 1 (1963) 177.
[25] T. Wagner, J. Optoelec. Adv. Mater. 4 (2002) 717.
[26] V.K. Saraswat, K. Singh, N.S. Saxena, Ind. J. Pure Appl. Phys. 44 (2006) 782.
[27] Mainika, P. Sharma, N. Thakur, Philos. Mag. 89 (2009) 3027.
[28] Deepika, P.K. Jain, K.S. Rathore, N.S. Saxena, J. Non-Cryst. Solids 355 (2009) 1274.
[29] M.K. El-Mously, M.M.El. Zaidia, J. Non-Cryst. Solids 27 (1978) 265.
[30] M. Lasocka, Mater. Sci. Eng. 23 (1976) 173.
[31] H.E. Kissinger, J. Res. Nat. Bur. Stand. 57 (1956) 217.
[32] K. White, R.L. Crane, J.A. Snide, J. Non-Cryst. Solids 103 (1988) 210.
[33] N.H. March, R.A. Street, M. Tosi, Amorphous Solids and Liquid State, Plenum, New York, 1985, pp. 434.
[34] M.M.A. Imran, D. Bhandari, N.S. Saxena, Physica B 293 (2001) 394.
[35] N.S. Saxxena, J. Non-Cryst. Solids 345–346 (2004) 161.
[36] A.A. Soliman, Therm. Acta 423 (2004) 71.
[37] M.A. Abdel Rahim, Physica B 322 (2002) 252.
[38] K. Matusita, T. Komatsu, R. Yokota, J. Mater. Sci. 19 (1984) 291.
[39] M.M.A. Imran, D. Bhandari, N.S. Saxena, Mater. Sci. Eng. A 292 (2000) 56.
[40] A.K. Singh, K. Singh, Philos. Mag. 89 (2009) 1457.
[41] Deepika, K.S. Rathore, N.S. Saxena, J. Phys. Condens. Matter 21 (2009), 335102 (8pp).
[42] G. Kaur, T. Komatsu, J. Mater. Sci. 36 (2001) 4531.
[43] R.M. Mehera, G. Kaur, P.C. Mathur, J. Mater. Sci. 26 (1991) 3433.
[44] N.B. Maharajan, N.S. Saxena, D. Bandari, M.M. Imran, D.D. Paudyal, Phys. Stat. Sol. (b) 23 (2000) 369.
[45] Y.Q. Gao, W. Wang, J. Non-Cryst. Solids 81 (1986) 129.
[46] J.A. Augis, J.E. Bennett, J. Therm. Anal. Calor. 13 (1978) 283.
[47] A.A. Elabbar, J. Alloys Compd. 476 (2009) 125.
[48] K.A. Aly, A.A. Othman, A.M. Absousehly, J. Alloys Compd. 467 (2009) 417.